



โครงการ
การเรียนการสอนเพื่อเสริมประสบการณ์

ชื่อโครงการ การสังเคราะห์ตัวเร่งปฏิกิริยาโลหะทรานซิชันไททานอสิลิเกตเพื่อใช้ใน
ปฏิกิริยาออกซิเดชัน
Synthesis of Transition Metal-Titanosilicate Catalyst for Oxidation
Reaction

ชื่อนิสิต นางสาวสาวิตรี เพ็งบุญ

ภาควิชา เคมี

ปีการศึกษา 2560

คณะวิทยาศาสตร์ จุฬาลงกรณ์มหาวิทยาลัย

Synthesis of Transition Metal-Titanosilicate Catalyst for Oxidation
Reaction

การสังเคราะห์ตัวเร่งปฏิกิริยาโลหะทรานซิชันไททานิลเกตเพื่อใช้ในปฏิกิริยา
ออกซิเดชัน

By

Miss Savitree Phengboon

A Senior Project Submitted in Partial Fulfillment of the
Requirements for The Degree of Bachelor of Science
Department of Chemistry, Faculty of Science
Chulalongkorn University
Academic Year 2017

Thesis Title Synthesis of Transition Metal-Titanosilicate Catalyst for Oxidation Reaction
By Miss Savitree Phengboon

Accepted by the Department of Chemistry, Faculty of Science, Chulalongkorn University in
Partial Fulfillment of the Requirements for the Bachelor Degree

SENIOR PROJECT COMMITTEE

P. Padungroa Chairman
(Assistant Professor Panuwat Padungroa, Ph.D.)

Duangamol Tungasmita Senior Project Advisor
(Duangamol Tungasmita, Ph.D.)

พรหมพงษ์ ปิ่นปิ่นจัทรม Examiner
(Assistant Professor Prompong Pienpinijtham, Ph.D.)

This report has been approved by the Head of Department of Chemistry

..... Head of Department of Chemistry
(Associate Professor Vudhichai Parasuk, Ph.D.)

Day May 2018

Writing quality of this report Excellent Good Medium

ชื่อโครงการ การสังเคราะห์ตัวเร่งปฏิกิริยาโลหะแทรนซิชันไททานิลิกेटเพื่อใช้ในปฏิกิริยาออกซิเดชัน

ชื่อนิสิตในโครงการ นางสาวสาวิตรี เฟ็งบุญ เลขประจำตัว 5733172823

ชื่ออาจารย์ที่ปรึกษา อาจารย์ ดร.ดวงกมล ตุงคะสมิต

ภาควิชาเคมี คณะวิทยาศาสตร์ จุฬาลงกรณ์มหาวิทยาลัย ปีการศึกษา 2560

บทคัดย่อ

ในงานวิจัยนี้สามารถสังเคราะห์ตัวเร่งปฏิกิริยาโลหะแทรนซิชันไททานิลิกेट (วานเดียมไททานิลิกेट-1 และ วานเดียมไททานเนียม-เอ็มซีเอ) ได้สำเร็จโดยวิธีทางความร้อน และตามด้วยวิธีเคลือบฝัง โดยผลิตภัณฑ์ที่สังเคราะห์ได้ทั้งหมดถูกตรวจสอบลักษณะทางกายภาพโดยใช้เทคนิคการเลี้ยวเบนของรังสีเอ็กซ์ การดูดกลืนแสงยูวี การดูดซับแก๊สไนโตรเจน กล้องจุลทรรศน์อิเล็กตรอนแบบส่องกราด และไอซีพี-ไออีเอส หลังจากที่มีการเคลือบฝังโลหะวานเดียมแล้วตัวเร่งปฏิกิริยาทั้งสองยังคงโครงสร้างของวัสดุต้นแบบไว้ได้ซึ่งสามารถยืนยันด้วยเทคนิคการเลี้ยวเบนของรังสีเอ็กซ์ และกล้องจุลทรรศน์อิเล็กตรอนแบบส่องกราด นอกจากนี้สถานะของวานเดียมออกไซด์สามารถพิสูจน์ได้ด้วยเทคนิคการดูดกลืนแสงยูวี พบว่าวานเดียมอยู่ในรูปของวานเดียมออกไซด์ (V_2O_5) ตัวเร่งปฏิกิริยาที่เตรียมนำไปทดสอบความสามารถในการเร่งปฏิกิริยาด้วยปฏิกิริยาออกซิเดชันของเบนซีนและแนฟทาลีนโดยมีไฮโดรเจนเปอร์ออกไซด์เป็นตัวออกซิไดซ์ จากผลการทดลอง พบว่าในบรรดาตัวเร่งปฏิกิริยาทั้งหมด วานเดียมไททานเนียม-เอ็มซีเอ มีความสามารถในการเร่งปฏิกิริยาได้ดีที่สุด มีการเปลี่ยนของแนฟทาลีนที่ 34.0 เปอร์เซ็นต์ และการเกิดผลิตภัณฑ์ฟินอล 14.0 เปอร์เซ็นต์

คำสำคัญ: ไทเทเนียมซิลิเกต, ตัวเร่งปฏิกิริยา, ปฏิกิริยาออกซิเดชัน, วิธีเคลือบฝัง

Project Title Synthesis of Transition Metal-Titanosilicate Catalyst for Oxidation
Reaction

Student Name Miss Savitree Phengboon Student ID 5733172823

Advisor Name Duangamol Tungasmita, Ph.D.

Department of Chemistry, Faculty of Science, Chulalongkorn University, Academic Year 2017

Abstract

The transition metal-titanosilicate catalysts (V/TS-1 and V/Ti-MCA) were successfully synthesized by hydrothermal treatment followed by impregnation method. All prepared catalysts were characterized by X-ray powder diffraction (XRD), DR-UV spectroscopy, N₂ adsorption-desorption, scanning electron microscopy-energy dispersive X-ray spectroscopy (SEM-EDX) and inductively coupled plasma-optical emission spectrometry (ICP-OES). After vanadium addition, the structural of two catalysts were still similar to parent materials confirming by XRD and SEM-EDX. Additionally, the vanadium particles in catalyst were vanadium oxide (V₂O₅) phase proved by DR-UV technique. The catalytic activity of the prepared catalysts was evaluated in the oxidation reaction of benzene and naphthalene with hydrogen peroxide as the oxidizing agent. From the results, among all catalysts, V/Ti-MCA provided the best catalytic efficiency with the naphthalene conversion as 34.0% and the yield of phenol as 14.0%.

Keywords: Titanosilicate, Catalysts, Oxidation reaction, impregnation

ACKNOWLEDGEMENTS

I would like to express my very great appreciation to my senior project advisor, Dr. Duangamol Tungasmita, for her valuable suggestion and support during this study.

I am particularly grateful for the assistance given by the chairperson, Assistant Professor Dr. Panuwat Padungros, for his kindness and advice in this project.

I would like to offer my special thanks to the examiner, Assistant Professor Dr. Prompong Peinpinijtham, for his help and useful advice.

I would like to thank Dr. Duangkamon Jiraroj, for her help in doing GC analysis and help me calculate the yield and conversion.

I would like to thank Miss Isara Mongkolpichayarak, for her help in doing ICP-OES analysis.

Finally, I wish to acknowledge Faculty of Science, Chulalongkorn University for the financial support and Department of Chemistry, Chulalongkorn university for valuable knowledge and experience.



CONTENTS

	PAGE
ABSTRACT IN THAI	iii
ABSTRACT IN ENGLISH	iv
ACKNOWLEDGEMENTS	v
CONTENTS	vi
LIST OF TABLES	ix
LIST OF FIGURES	x
LIST OF SCHEMES	xi
LIST OF ABBREVIATION	xii
CHAPTER I INTRODUCTION	1
1.1 Background	1
1.2 Literature reviews of benzene oxidation	2
1.3 Literature reviews of naphthalene oxidation	3
1.4 Theory	4
1.4.1 Catalysts	4
1.4.1.1 Types of catalysts	4
1.4.1.1.1 Homogeneous catalysts	4
1.4.1.1.2 Heterogeneous catalysts	4
1.4.1.2 Porous materials	5
1.4.1.2.1 Microporous materials	5
1.4.1.2.1.1 Titanium silicate-1 (TS-1)	5
1.4.1.2.2 Mesoporous materials	6
1.4.1.2.2.1 Mesoporous Cubic <i>1a-3d</i> Amorphous(MCA)	6
1.4.2 Characterization of catalysts	6
1.4.2.1 X-ray diffraction	6
1.4.2.2 Diffuse reflectance UV-Vis spectroscopy (DR-UV)	7
1.4.2.3 N ₂ adsorption-desorption technique	8
1.4.2.4 Scanning electron microscopy (SEM)	8
1.4.2.5 Energy dispersive X-ray spectroscopy (EDX)	9

1.4.2.5 Inductively coupled plasma-optical emission spectrometry(ICP-OES)	9
1.4.3 Oxidation Reaction	10
1.5 Objectives	10
CHAPTER II EXPERIMENTAL	11
2.1 Chemicals	11
2.2 Catalysts preparation	12
2.2.1 Titanium silicate-1 (TS-1) preparation	12
2.2.2 Ti-MCA preparation	14
2.2.3 Bimetallic catalyst preparation	15
2.3 Catalyst characterization	15
2.3.1 X-ray diffraction	15
2.3.2 DR-UV spectroscopy	13
2.3.3 Surface area analyzer	16
2.3.4 Scanning electron microscopy (SEM)	16
2.3.5 Inductively coupled plasma-optical emission spectrometry(ICP-OES)	16
2.4 Procedure in oxidation reaction of benzene	17
2.5 Procedure in oxidation reaction of naphthalene	17
2.6 Iodometric titration process	17
2.6.1 Standardization of Sodium Thiosulfate	17
2.6.2 Determination of Hydrogen Peroxide	18
2.7 Gas chromatography analysis (GC)	18
CHAPTER III RESULTS AND DISCUSSION	20
3.1 Catalysts characterization	20
3.1.1 X-ray diffraction	20
3.1.1.1 TS-1	20
3.1.1.2 Ti-MCA	21
3.1.2 DR-UV results	22
3.1.3 N ₂ sorption properties	23
3.1.3.1 TS-1	23
3.1.3.2 Ti-MCA	24
3.1.4 SEM images	25
3.1.5 ICP-OES results	27
3.2 Oxidation reaction of benzene and naphthalene	27

CHAPTER IV CONCLUSIONS

29

REFERENCES

30

APPENDICES

33

VITAE

35



LIST OF TABLES

Table 1.1 IUPAC classification of porous materials	5
Table 1.2 Classification of mesoporous materials	6
Table 2.1 The operational parameters of X-ray powder diffractometer	16
Table 3.1 Textural properties of vanadium supported of TS-1 and Ti-MCA materials	25
Table 3.2 Metal content analysis of V/TS-1 and V/Ti-MCA with different V-content	27
Table 3.3 Catalytic activity of transition metal-titanosilicate for the oxidation reaction of benzene and naphthalene	28



LIST OF FIGURES


Figure 1.1 Uses of phenol	1
Figure 1.2 Cumene process	2
Figure 1.3 Energy profile diagram of reaction with and without catalyst	4
Figure 1.4 (a) MFI structure and (b) 10-membered ring channels in MFI	6
Figure 1.5 Diffraction of X-rays by regular planes of atoms	7
Figure 1.6 The IUPAC classification of adsorption isotherm	8
Figure 1.7 The main process of scanning electron microscope	9
Figure 1.8 Major components and ICP-OES instrument	10
Figure 3.1.1 XRD patterns of bimetallic titaniumsilicalite-1 (V/TS-1) in the range of low-angle	20
Figure 3.1.2 XRD patterns of bimetallic titaniumsilicalite-1 (V/TS-1) in the range of wide-angle	21
Figure 3.2 XRD patterns of bimetallic Ti-MCA (V/Ti-MCA) in the range of (a) low-angle and (b) wide-angle	22
Figure 3.3 DR-UV spectra of V/TS-1 and V/Ti-MCA	23
Figure 3.4 N ₂ adsorption/desorption isotherms of bimetallic TS-1	24
Figure 3.5 N ₂ adsorption/desorption isotherms of bimetallic Ti-MCA.	25
Figure 3.6 The SEM image and EDX map composite element Ti, V, Si, O of (a) V/TS-1, (b) V/a-TS-1, (c) V/Ti-MCA and (d) V/a-Ti-MCA	26
Figure A-1 Calibration curve of phenol	34
Figure A-2 Calibration curve of naphthalene	34

LIST OF SCHEMES

Scheme 2.1 Diagram of titanium silicate-1 preparation.	13
Scheme 2.2 Diagram of Ti-MCA preparation	14
Scheme 2.3 Diagram of bimetallic catalyst preparation.	15
Scheme 2.4 The temperature program of benzene used for Gas chromatography analysis.	18
Scheme 2.5 The temperature program of naphthalene used for Gas chromatography analysis.	19



LIST OF ABBREVIATION



Å	Angstrom unit
BET	Brunauer-Emmett-Teller
BJH	Barret-Joyner-Halender
°C	Degree Celsius
g	Gram
GC	Gas chromatography
h	Hour or hours
l	lilite
kV	Kilovolt
M	Molar
N	Normality
min	Minute or minutes
mg	Milligram (s)
ml	Milliliter (s)
nm	Nanometer (s)
SEM	Scanning electron microscopy
wt.%	Percent by weight
XRD	X-ray diffraction

CHAPTER I

INTRODUCTION

1.1 Background

Phenol and phthalic anhydride are important industrial chemicals widely used in plastics and so on [1]. The demand in the global phenol and phthalic anhydride market is substantially influenced by general macroeconomic factors and thus, the consumption of phenol and phthalic anhydride was a direct relation to the growth patterns of major world economies as shown in Figure 1.1.

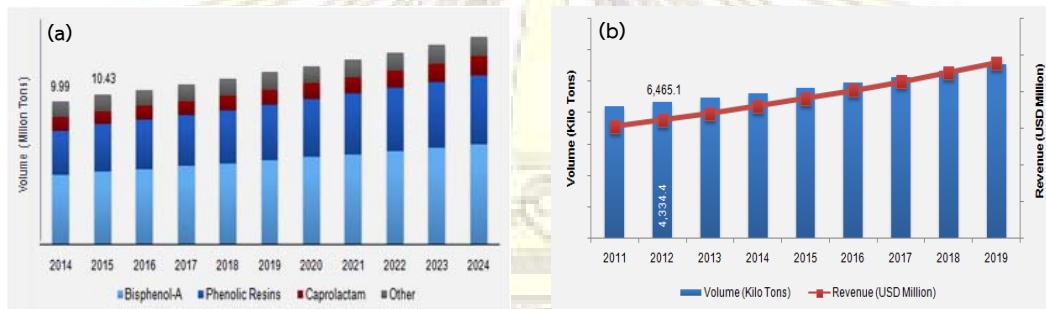


Figure 1.1 The global market of (a) phenol and (b) phthalic anhydride [2]

The vast majority of phenol is made by the cumene process while the processes for producing phthalic anhydride use *o*-xylene or naphthalene with dioxygen. However, the disadvantages of the cumene process are not only consisting of multistage in the process but also providing an equimolar amount of acetone as by-product that exceeds market demand as shown in Figure 1.2. Moreover, this cumene process produces the explosive intermediate and requires the complicated equipment which results in a high cost process. In addition, the disadvantage for producing phthalic anhydride is high temperature. In order to overcome these problems, a process for the direct oxidation of benzene to phenol and oxidation of naphthalene to phthalic anhydride with hydrogen peroxide will be studied.

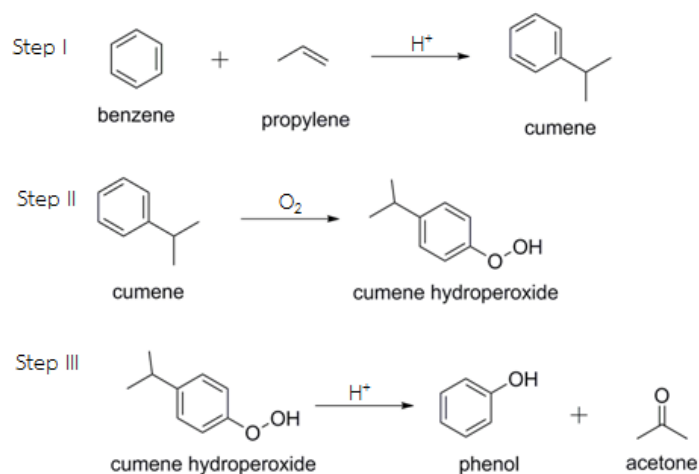


Figure 1.2 Cumene process [1]

1.2 Literature reviews of benzene oxidation

In 2013, XU Dan *et al* [3] studied liquid phase hydroxylation of benzene to phenol with hydrogen peroxide over VO_x - TiO_2 catalyst samples with Cu as a second metal. A series of Cu/VO_x - TiO_2 (vanadium loading was 4.3%) catalysts was prepared within the range of Cu loading (0.29%–2.5%) and calcined at the temperatures of 350–650 °C. The effects of Cu loading, catalyst amount, and reaction temperature on the catalytic performance were also studied in reaction. From the results, the $Cu(0.75)/V(4.3)TiO_2$ -450 catalyst had high catalytic activity for the hydroxylation of benzene to phenol, and gave a phenol yield of 26% and phenol selectivity of 92%.

In 2014, Xiangju Y. *et al* [4] studied selective oxidation of benzene to phenol by Fe-CN/titanium silicate-1(TS-1) catalysts under visible light irradiation. The Fe- γ - C_3N_4 (denoted as Fe-CN) and TS-1 hybrid materials were fabricated by a facial thermal polymerization approach using dicyandiamide, metal chloride as precursors and TS-1 zeolite as a support. From the results, it was found that the Fe-CN/TS-1 hybrid materials showed superior photocatalytic performance for the phenol production from benzene to sole Fe-CN and TS-1 catalysts. Under the optimal conditions, up to 10.0% phenol yield (based on benzene) was achieved over the hybrid materials, with 18.4% phenol selectivity (based on H_2O_2).

In 2015, Yuma M. *et al* [5] studied selective hydroxylation of benzene to phenol with H_2O_2 in the presence of a catalytic amount of the nickel complex at 60 °C. From the results, the maximum yield of phenol was 21% based on benzene without the formation of quinone or diphenol. The total turnover number of the nickel complex supported by tris[2-(pyridin-2-yl)ethyl]amine reached 749, which is the highest value ever reported for molecular

catalysts. The aromatic hydroxylation method has been shown to be applicable to oxygenation of alkylbenzene derivatives. The selectivity for cresol in the toluene hydroxylation reached 90%, which is also the highest reported value for direct hydroxylation of toluene to cresol with H_2O_2 and a molecular catalyst.

1.3 Literature reviews of naphthalene oxidation

In 2007, F. Shi *et al* [6] studied selective oxidation of naphthalene derivatives with ruthenium catalysts using hydrogen peroxide as terminal oxidant and water as the solvent. The effect of different ruthenium complexes, phase transfer catalysts, and the concentration of hydrogen peroxide were studied. From the results, the selective oxidation of naphthalene gave the desired naphthoquinone in 39–59% isolated yield.

In 2009, Adrienn B. *et al* [7] studied selective oxidation of condensed cyclic aromatics (naphthalene, tetralin and decalin) with hydrogen peroxide in the presence of Ti, Fe or Cr containing MCM-41 and SBA-15 mesoporous catalysts. Using ultrasonic equipment, both in methanol and acetonitrile solvent, formation of naphthols could be detected in the oxidation of naphthalene. From the results, the Cr-MCM-41 showed the best catalytic performance in the oxidation of tetralin with hydrogen peroxide, the 1-tetralone selectivity have reached over 30% and there are 30% conversion.

In 2017, Zhiwei Z. *et al.* [8] studied liquid-phase oxidation of naphthalene with H_2O_2 in the presence of ordered mesoporous $V\text{-}m\text{-Al}_2\text{O}_3$ catalysts. The $V\text{-}m\text{-Al}_2\text{O}_3$ catalysts were successfully synthesized *via* a facile one-pot evaporation-induced self-assembly (EISA) method. The $8V\text{-}m\text{-Al}_2\text{O}_3$ catalyst shows higher catalytic performance than other samples owing to its highest surface area, appropriate pore volume and size, whose naphthalene conversion and phthalic anhydride selectivity are 45.4% and 61.0%, respectively.

The benzene and naphthalene oxidation by using hydrogen peroxide as the oxidant provides high conversion but low selectivity. Another advantage of hydrogen peroxide is its comparatively low cost. From an economic and environmental standpoint, hydrogen peroxide is chosen as the good oxidizing agent. Moreover, many transition metals such as Cu, Fe, Cr, Ti and V were used to catalyze the oxidation of benzene and naphthalene. In this work, Ti is selected as the main element for synthesis of microporous and mesoporous titanoliscates, which is one of the high potential catalysts in oxidation field. The vanadium metal is a second metal in order to improve catalytic activity of catalysts. The synthesized catalysts are tested in benzene and naphthalene oxidation reaction using hydrogen peroxide as oxidizing agent.

1.4 Theory

1.4.1 Catalysts

A catalyst is a compound that accelerates the progress of a reaction without being consumed. When the reaction has finished, the mass of catalyst is the same as at the beginning. Moreover, it does not affect the equilibrium state of a reaction. In addition, the catalyst may capacitate the reaction at low temperature, or expand reaction rate or selectivity. An energy profile of reaction with and without catalyst is illustrated in Figure 1.3.

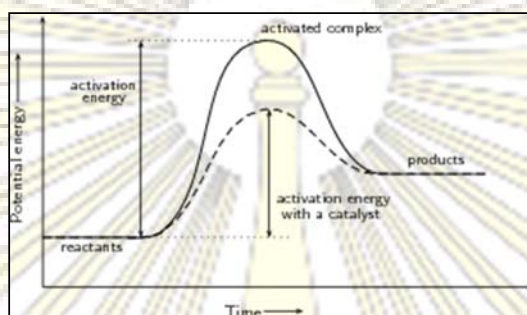


Figure 1.3 Energy profile diagram of reaction with and without catalyst [9]

1.4.1.1 Types of catalysts

Catalysts can be divided into two main types, heterogeneous and homogeneous catalysts [10].

1.4.1.1.1 Homogeneous catalysts

In homogeneous catalysis, this has the catalyst in the same phase as the reactants. Typically, everything will be present as a gas or contained in a single liquid phase. An advantage of homogeneous catalysis is that the catalyst can be mixed into the reaction mixture, allowing a very high degree of interaction between catalyst and reactant molecules. However, the major drawback of homogeneous catalyst is the difficulty of their recovery from the product.

1.4.1.1.2 Heterogeneous catalysts

In heterogeneous catalysis is a type of catalysis in which the catalyst occupies a different phase from the reactants and products. Because of this, it cannot be mixed in with the reactants. Although heterogeneous catalysts exhibit a lower activity than homogeneous catalyst, the use of heterogeneous catalysts is always advantageous from both environmental and economic points of view due to its efficient recycling and easy handling.

1.4.1.2 Porous materials

A molecular sieve is a material with pores of uniform size that exhibited absorption properties which can be classified on the IUPAC definitions into three main types depending on their pore size. Properties and examples of these materials are given in Table 1.1.

Table 1.1 IUPAC classification of porous materials [11].

Type of porous molecular sieve	Pore size (nm)	Example
Microporous material	<2	ZSM-5, TS-1
Mesoporous material	2-50	Ti-MCA, MCM-41, SBA-15
Macroporous material	>50	Glasses

1.4.1.2.1 Microporous materials

Microporous are occasionally classified into smaller size ultramicropores (less than 0.7 nm) and supermicropores that are larger than ultramicropores but smaller than mesopores. Microporous materials include carbon absorbents, silica gels, zeolites, etc.

1.4.1.2.1.1 Titanium silicate-1 (TS-1)

Titanium silicalite-1 (TS-1), discovered for the first time in 1983 by Taramasso et al., is a material with MFI structure. The MFI structure is built up by 5-1 secondary building units which are link together to form chain and interconnection of this chains leading to the formation of the channel system in the structure [12]. Figure 1.4 illustrates MFI structure and 10-membered ring channels in MFI. The MFI-type structure has a three dimensional pore system, which is a combination of sinusoidal (zigzag) 10-membered ring channels (0.51-0.55 nm), that directed along the a-axis, and the intersecting straight 10-membered ring channels (0.54-0.56 nm) that run parallel to the b-axis of the orthorhombic unit cell. The catalytic activity of TS-1 is associated with the isolated Ti^{4+} ions that present into the MFI framework as T-atoms. For the application, the main use of TS-1 is in the oxidation reaction of alkanes, alkenes and aromatic hydrocarbons in the presence of hydrogen peroxide [13, 14].

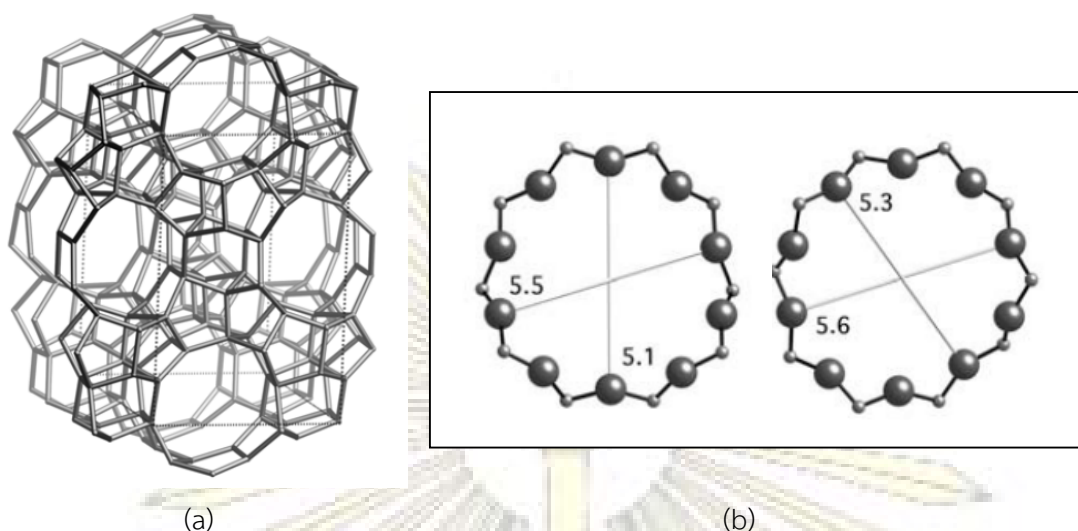


Figure 1.4 (a) MFI structure and (b) 10-membered ring channels in MFI

1.4.1.2.2 Mesoporous materials

Mesoporous materials can be classified by different synthetic methods, as shown in Table 1.2.

Table 1.2 Classification of mesoporous materials

Assembly	Template	Media	Material
Electrostatic	Quaternary ammonium salt	Base or acid	MCM-41
H-bonding	Primary amine	Neutral	HMS
H-bonding	Amphiphilic triblock copolymer	Acid (pH<2)	SBA-15

1.4.1.2.2.1 Mesoporous Cubic $la-3d$ Amorphous (MCA)

Large-pore mesoporous silica with cubic $la-3d$ has been synthesized by using triblock copolymer Pluronic 123 as a template [15]. The cubic $la3d$ mesoporous silica (MCA) has a three-dimensional (3D) structure similar to MCM-48, which was synthesized by using cetyltrimethylammonium bromide (CTAB) as the template [16].

1.4.2 Characterization

1.4.2.1 X-ray diffraction

X-ray diffraction (XRD) is an instrumental technique to study the atomic spacing and crystal structure. Moreover, it can be used for the study of component in samples. XRD can provide additional information beyond basic identification. In general, crystal diffracts the

X-ray beam differently, depending on its structure and orientation. The diffracted X-ray is collected by an area detector. The diffraction pattern consists of reflections of differently intensity which can be used to determine the structure of the crystal by the Bragg equation. Figure 1.5 shows diffraction of X-ray by regular planes of atoms. Bragg's law is able to determine the interplanar spacing of the samples, from diffraction peak according to Bragg angle.

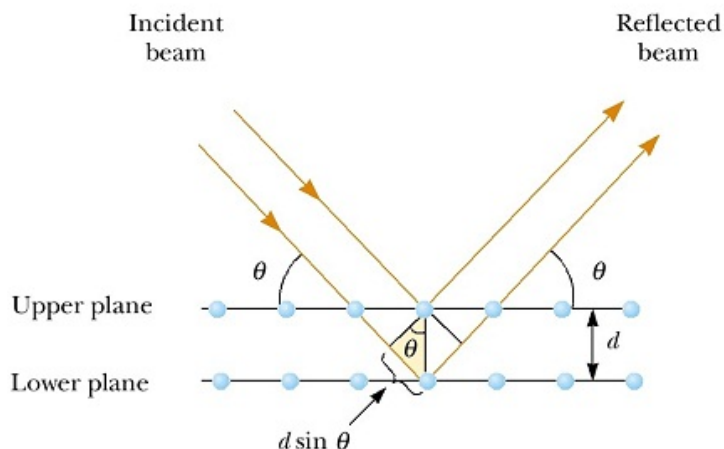


Figure 1.5 Diffraction of X-rays by regular planes of atoms [17]

$$n\lambda = 2d \sin\theta$$

Where n is the integer, λ is the wavelength, d is the distance between equivalent atomic planes and θ is the angle of between the incident beam and these planes.

1.4.2.2 Diffuse reflectance UV-Vis spectroscopy (DR-UV)

The DR-UV spectrometer is the instrument, which provides information on the electronic structure of molecules, the valence and coordination of metal cations. The DR-UV spectrometer was used to study oxidation state of various metals containing in catalysts. The UV-Vis spectrum can give information about the oxidation state, the environmental symmetry of transition metal ions, (e.g., tetrahedrally or octahedrally coordinated ions), and the degree of polymerization. The solid sample in form of powders are measured in reflectance mode owing to low transparency which the DR-UV-Vis spectrum can be described by the Kubelka-Munk function $F(R_{\infty})$:

$$F(R_{\infty}) = (1 - R_{\infty})^2 / 2R_{\infty} = k/s$$

Where $F(R_{\infty})$ is usually termed the reemission or Kubelka-Munk (K-M) function, R_{∞} is the diffuse reflection of the sample, K and S are the absorption and scattering coefficient of the sample, respectively.

1.4.2.3 N₂ adsorption-desorption technique

N₂ adsorption-desorption technique is used to determine surface area, pore volume, pore diameter and pore size distribution of material. According to IUPAC, adsorption-desorption isotherms are classified into six types, as shown in Figure 1.6. The type of adsorbate and type of adsorbents including intermolecular interaction between gas and surface influence the type of isotherms. The isotherm type I is microporous. Type II shows the isotherm for nonporous while type III is typical behavior for macroporous or nonporous materials owing to a relatively weak interaction between adsorbate and adsorbent. The isotherm type IV is mesoporous. The isotherm type V is porous materials and materials that have the weak interaction between the adsorbate and adsorbent. The isotherm type VI is homogeneous surface materials.

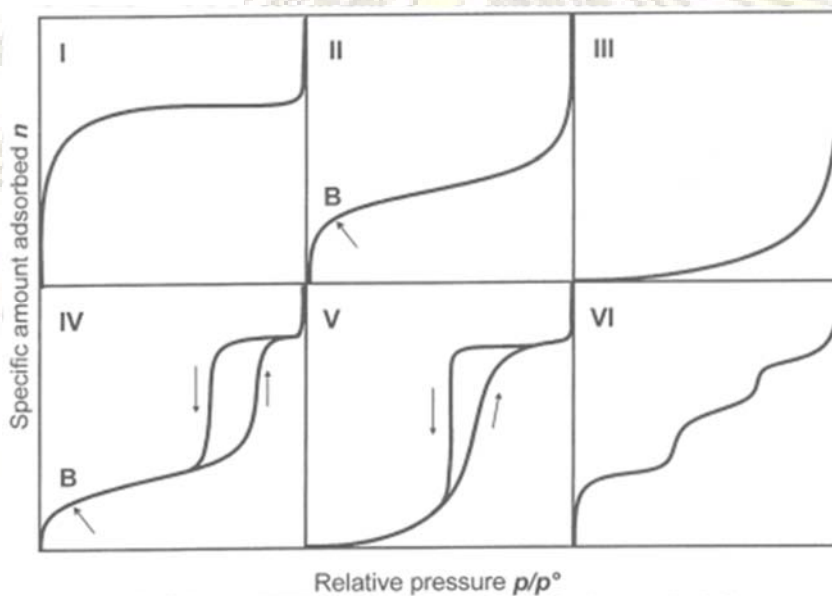


Figure 1.6 The IUPAC classification of adsorption isotherm [18]

1.4.2.4 Scanning electron microscopy (SEM)

Scanning electron microscopy (SEM) is a technique used to study morphology such as surface, size, and shape of particles. Moreover, it can be used to provide elemental identification and quantitative compositional information from energy dispersive X-ray spectroscopy (EDX). SEM uses a focused scanned electron beam to produce images of the sample. The electron interact with atom in the sample, producing various signal that can be detected and obtain information about surface and morphology of sample. The scanning electron micrograph results 3-dimension black and white images.

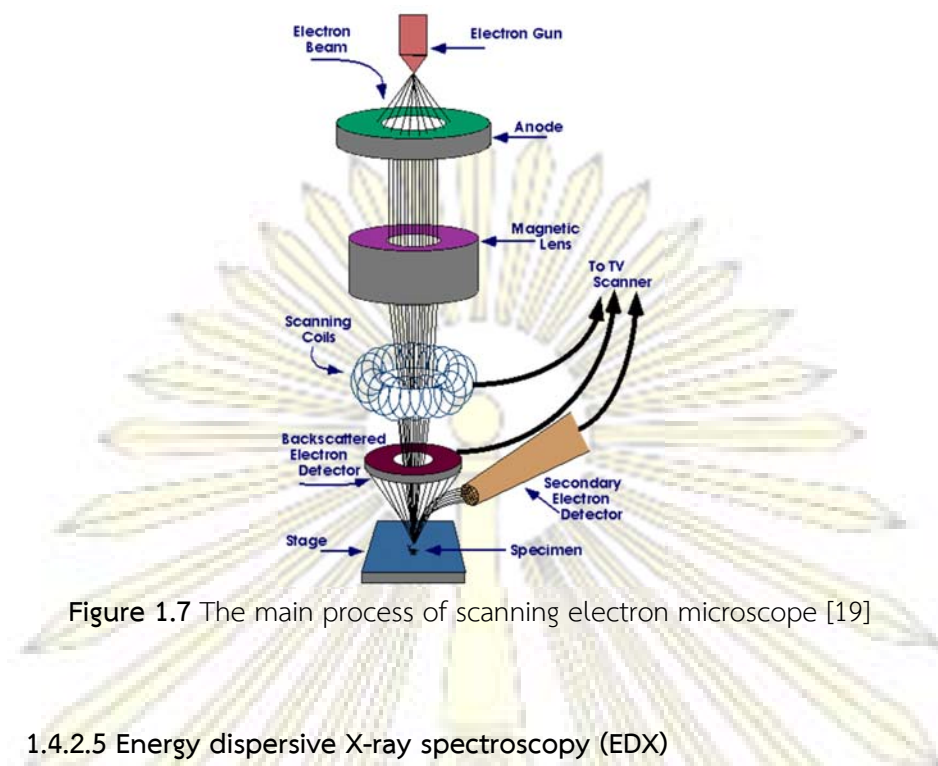


Figure 1.7 The main process of scanning electron microscope [19]

1.4.2.5 Energy dispersive X-ray spectroscopy (EDX)

Energy dispersive X-ray spectroscopy (EDX) is used to find the chemical composition of materials down to a spot size of a few microns, and to create element composition maps over a much broader raster area. Together, these capabilities provide fundamental compositional information for a wide variety of materials. When an incident beam electron strikes an atom, it may knock out an inner shell electron if the beam electron has sufficient energy. As the excited atom returns to its stable state, the excess energy is released as an X-ray photon or Auger electron. The emitted X-rays have characteristic energies for each specific atom, thus they provide chemical information about the sample.

1.4.2.6 Inductively coupled plasma-optical emission spectrometry (ICP-OES)

Inductively coupled plasma-optical emission spectrometry (ICP-OES) is a technique that use to find the composition of elements in samples can be determined using plasma and a spectrometer. According to principle of ICP-OES, The solution to analyze is conducted by a peristaltic pump through a nebulizer into a spray chamber. The produced aerosol is led into argon plasma. In the ICP-OES the plasma is generated at the end of a quartz torch by a cooled induction coil which a high frequency alternate current flows. As a consequence, an alternate magnetic field is induced which accelerated electrons into a circular trajectory. Due to collision between the argon atom and the electrons ionization occurs, giving rise to a stable plasma. The plasma is extremely hot, 6000-7000 K. In the

induction zone, it can even reach 10000 K. In the torch desolvation, atomization and ionizations of the sample takes place. Due to the thermic energy taken up by the electrons, they reach a higher excited state. When the electrons drop back to ground level energy is liberated as light. Each element has an own characteristic emission spectrum that is measured with a spectrometer. The light intensity on the wavelength is measured and with the calibration calculated into a concentration. A representation of the layout of a typical ICP-OES instrument is shown in Figure 1.8.

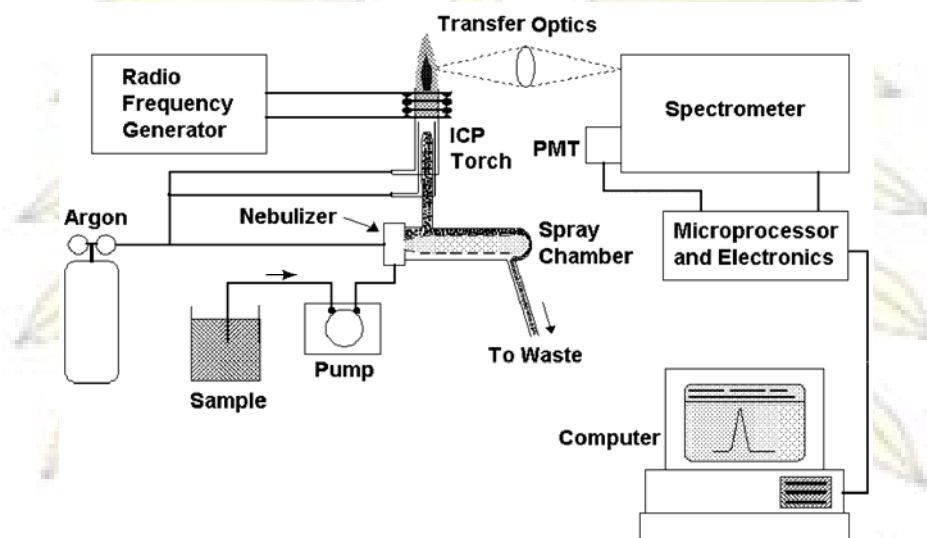


Figure 1.8 Major components and ICP-OES instrument [20]

1.4.3 Oxidation reaction

Oxidation reaction is a reaction which a molecule or a atom lose an electron to a receptor or an oxidizing agent. This reaction might relate to oxygen, however, losing of hydrogen atom from the molecule could be also an oxidation reaction [21].

1.5 Objectives

1.5.1 To synthesize transition metal-titanosilicate catalysts for oxidation reaction of benzene and naphthalene.

1.5.2 To test the catalytic activity of synthesized catalysts for oxidation reaction of benzene and naphthalene using hydrogen peroxide as an oxidant.

CHAPTER II

EXPERIMENTAL

2.1 Chemicals

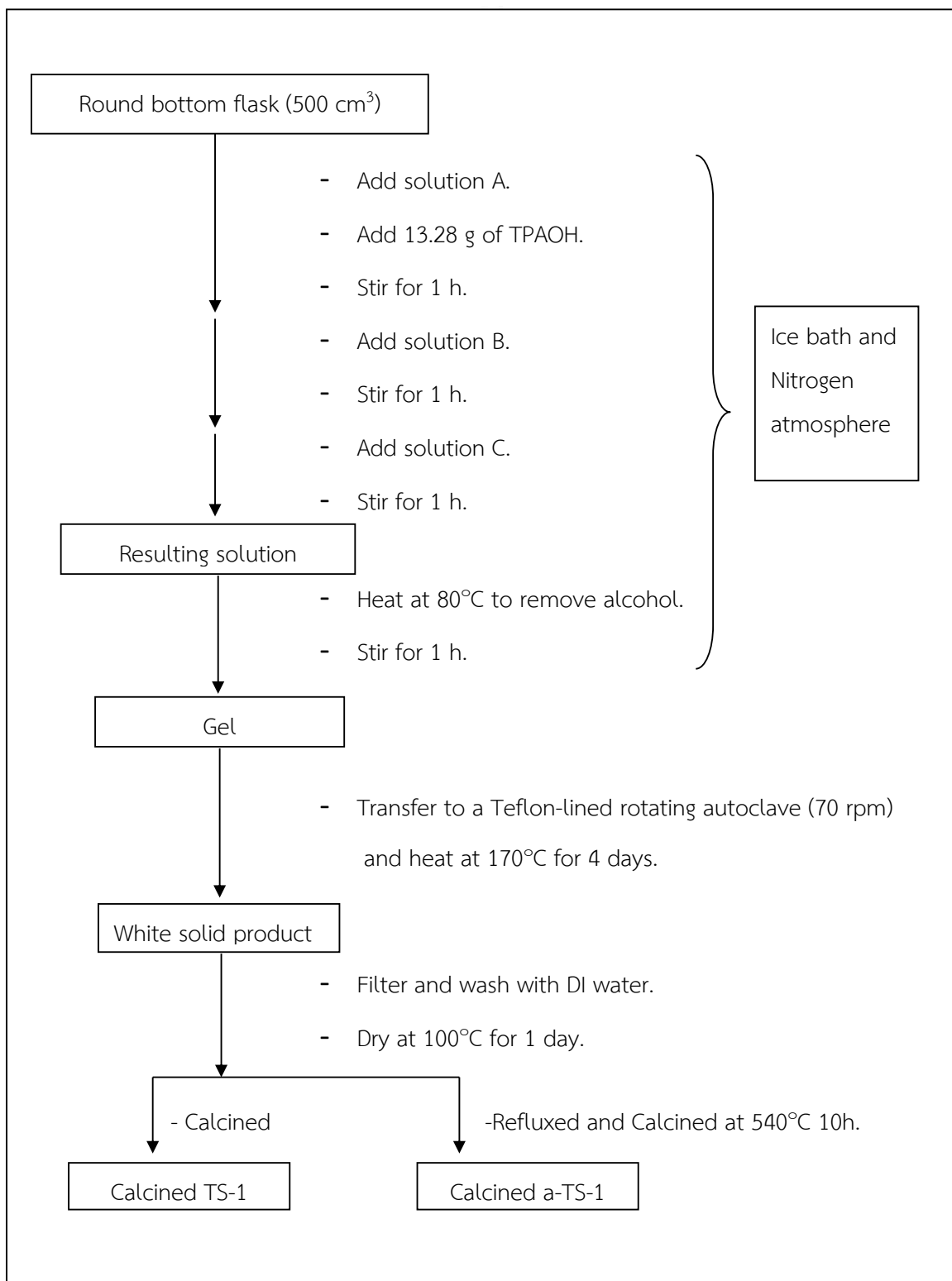
1. Hydrochloric acid, HCl (Merck, 37 wt.%)
2. Ethanol (Merck)
3. 3-(mercaptopropyl) trimethoxysilane, MPTMS (Aldrich, 95.0%)
4. Pluronic P123, PEO₂₀-PPO₇₀-PEO₂₀ (Aldrich)
5. Nitric acid, HNO₃ (Merck, 65%)
6. 2-propanol (Merck, 99.8%)
7. Tetrabutyl orthotitanate, TBOT (Aldrich, 97%)
8. Tetraethyl orthosilicate, TEOS (Fluka, 98%)
9. Tetrapropylammonium bromide, TPABr (Aldrich, 98%)
10. Tetrapropylammonium hydroxide, TPAOH (Merck, 40%)
11. Vanadium (III) chloride, VCl₃ (Merck, 99.0%)
12. Acetonitrile, CH₃CN (Fisher Scientific, 99.9%)
13. Titanium isopropoxide, TIP (Fluka, 97%)
14. Hydrogen peroxide, H₂O₂ (Merck, 30%)
15. Ammonium molybdate, (NH₄)₆Mo₇O₂₄·4H₂O (Baker Analyzed, 81.5%)
16. Potassium iodate, KIO₃ (Ajax Finechem, 99.4%)
17. Potassium iodide, KI (Carlo Erba, 99%)
18. Sodium hydroxide, NaOH (Merck, 99%)
19. Sodium thiosulfate, Na₂S₂O₃·5H₂O (Ajax Finechem, 99.5%)
20. Starch powder (Aldrich)
21. Sulfuric acid, H₂SO₄ (Merck, 95%)
22. Benzene, C₆H₆ (Carlo Erba, 99%)
23. Phenol, C₆H₅OH (Merck, 99%)
24. Cycloheptanone, C₇H₁₂O (Aldrich, 99%)
25. Tetrahydrofuran, THF (ACI Labscan, 99.8%)
26. Naphthalene, C₁₀H₈ (Fluka, 98%)

2.2 Catalysts preparation

2.2.1 Titanium silicate-1 (TS-1) preparation

In the preparation of TS-1 with Si/Ti = 40, using tetrapropylammonium hydroxide (TPAOH) and tetrapropyl-ammonium bromide (TPABr) as template, tetraethyl orthosilicate (TEOS) and tetrabutyl orthotitanate (TBOT) as the Si and Ti source respectively. The molar composition of the gel was 1 TEOS : 0.025 TBOT : 0.18 TPAOH : 0.18 TPABr : 7.56 2-PrOH : 36.35 H₂O [22]. Three aqueous solutions were prepared separately, Solution A was obtained by dissolving 37.82 g of TEOS in 66 g of 2-propanol. Solution B was prepared by dissolving 1.55 g of TBOT in 16.5 g of 2-propanol. Solution C was prepared by dissolving 8.89 g of TPABr in 59 g of deionized water and mixed with 53.16 g of TPAOH. In the ice bath and nitrogen atmosphere, 13.28 g of TPAOH was added dropwise into solution A with stirring for 1 h. After that, solution B was added dropwise into the mixture. After stirring for 1 h, solution C was added dropwise and the mixture was stirred for another 1 h. The resulting solution was heated at 80°C to remove alcohol. The solution was stirred for 1.5 h in air. Thereafter, the resulting gel was transferred to Teflon-lined autoclave and heated at 170°C for 4 days with rotated at 70 rpm. The solid product was washed with deionized water and dried at 100°C for 1 day. The solid product was divided into two parts. One of these was refluxed with 6 M HNO₃ at 100°C for 24 h and calcined. For another part of solid, solid product was calcined at 540°C for 10 h. The process for titanium silicalite-1 preparation was illustrated in Scheme 2.1.

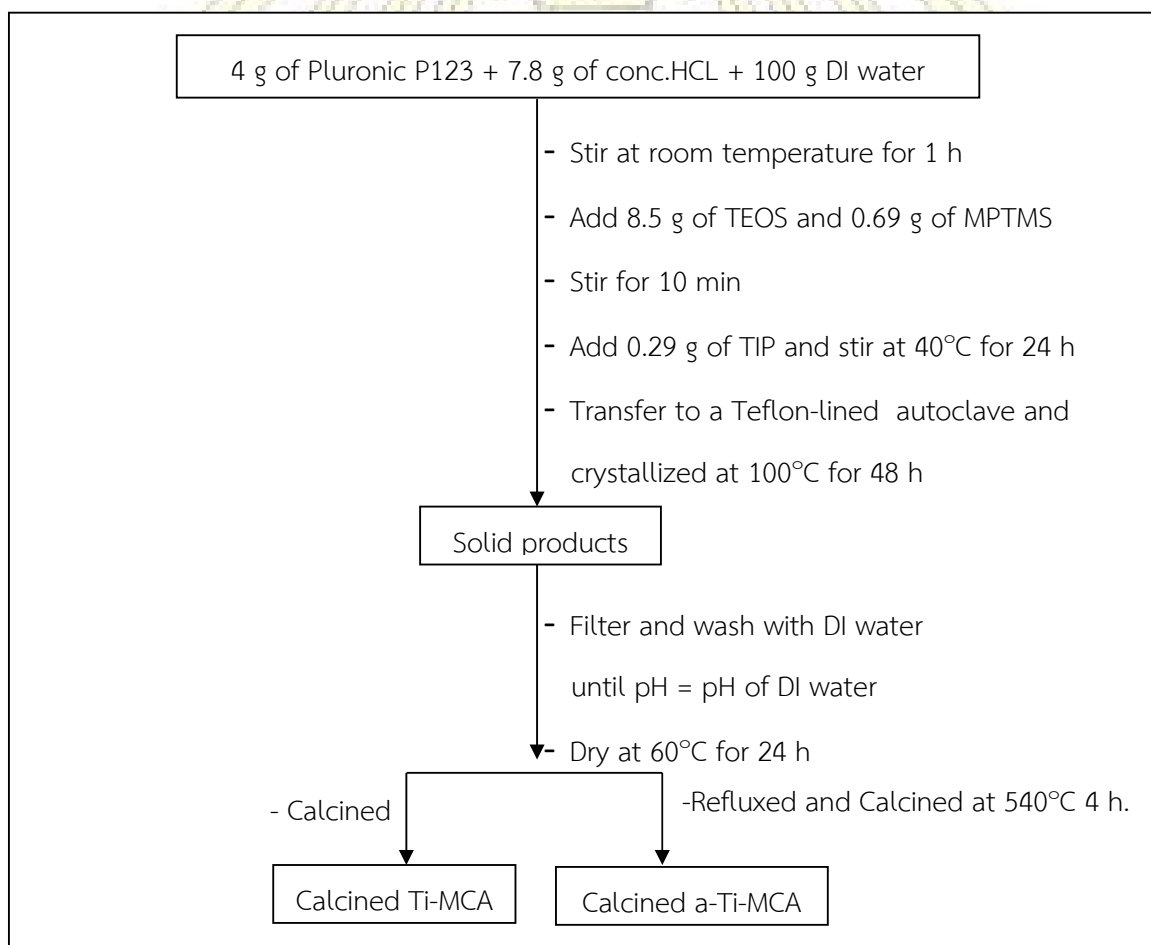




Scheme 2.1 Diagram of titanium silicate-1 preparation

2.2.2 Ti-MCA preparation

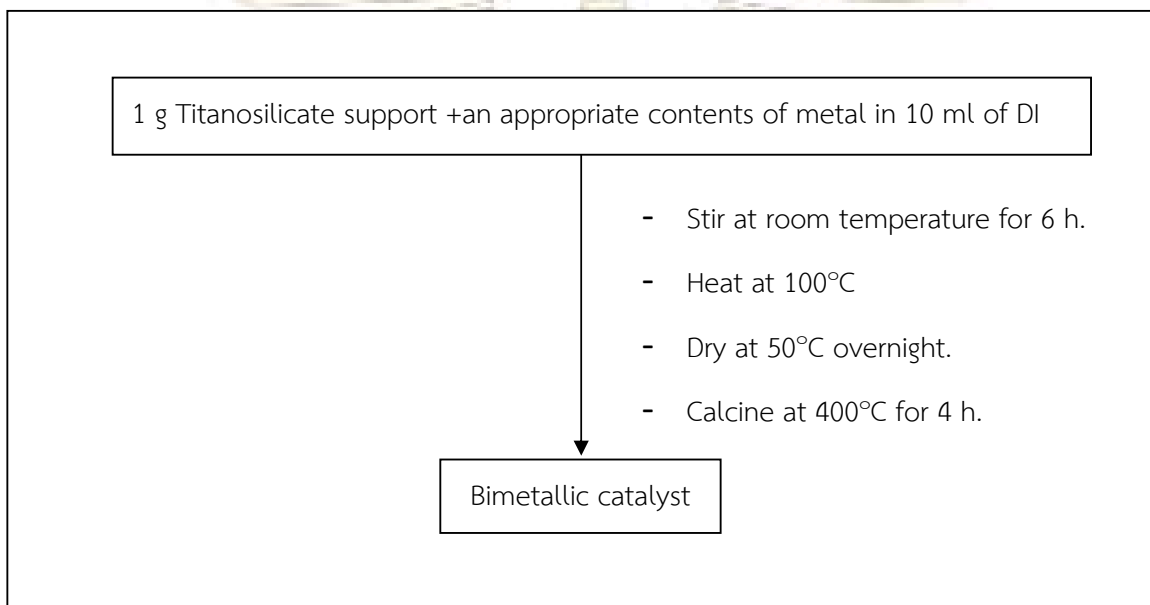
Ti-MCA was prepared by directly hydrothermal method modified from Kubota's method using pluronic P123 triblock copolymer as a structure directing agent, tetraethyl orthosilicate (TEOS) and titanium isopropoxide as the Si and Ti sources, respectively [23]. The molar gel composition of Ti-MCA with mole ratio of Si/Ti =40 was 1TEOS : 0.025 TIP : 0.018 P123 : 0.089 MPTMS : 2 HCL : 148 H₂O. In the procedure, 4 g of Pluronic P123 was added to 7.8 g of HCl and 100 g of deionized water. The mixture was stirred to homogeneous at room temperature for 1.5 h. After that, 8.5 g of TEOS and 0.69 g of MPTMS were added to the solution and stirred for 10 min. Then, 0.29 g of TIP was slowly added into the solution under vigorously stirred at 40°C for 24 h. The resulting solution was transferred to Teflon-lined autoclave and crystallized at 100°C for 48 h. The precipitated product was filtered, washed with deionized water until pH equal with pH of DI water, dried at 60°C for 24 h. The solid product was divided into two parts. One of these was refluxed with 6 M HNO₃ at 100°C for 24 h and calcined. For another part of solid, solid product was calcined at 550°C for 4 h. The procedure for synthesizing the Ti-MCA was shown in Scheme 2.2.



Scheme 2.2 Diagram of Ti-MCA preparation

2.2.3 Bimetallic catalyst preparation

10wt.% metal vanadium supported on titanosilicate supports (TS-1 and Ti-MCA) were prepared by wetness impregnation method from vanadium (III) chloride. The appropriate contents of metal was loaded at room temperature under stirring for 6 h. Afterwards, the mixture was heated at 100°C, dried at 50°C overnight and calcined at 400°C for 4 h. The resulting products were denoted as V/TS-1 and V/Ti-MCA. The procedure for preparing bimetallic catalyst was shown in Scheme 2.3



Scheme 2.3 Diagram of bimetallic catalyst preparation

2.3 Catalyst characterization

2.3.1 X-ray diffraction (XRD)

The X-ray diffraction patterns of synthesized catalysts were identified with a Rigaku Dmax 2200/Ultima+ X-ray diffractometer equipped with Cu target X-ray tube (40 kV, 30 mA). For the analysis of crystalline structure, the range of 2-theta, scan speed, scan step, scattering slit, divergent slit and receiving slit of all catalysts are shown in Table 2.1. The measured diffractograms were analyzed using Material Database Incorporation (MDI) software.

Table 2.1 The operational parameters of X-ray powder diffractometer.

Catalyst support	2-theta (degree)	Scan speed (degree/min)	Scan step (degree)	Scattering slit (degree)	Divergent slit (degree)	Receiving slit (mm)
TS-1	5-50	5	0.02	0.5	0.5	0.3
Ti-MCA	0.7-3	1	0.02	0.05	0.5	0.15

2.3.2 DR-UV spectroscopy (DR-UV)

The diffuse reflectance UV spectra were recorded in the range of 200-700 nm by a Shimadzu UV-2550 spectrophotometer with BaSO₄ as reference under ambient temperatures. The spectra of metal oxide species were collected in order to prove the metal position.

2.3.3 Surface area analyzer

Specific surface area, N₂ adsorption-desorption isotherms and pore size distribution of catalysts were determined by a BEL Japan, BELSORP-mini instrument. Before the measurement, 40 mg of calcined sample was weighed and pretreated at 180 °C for 3 h.

2.3.4 Scanning electron microscopy (SEM)

The morphology of synthesized catalysts was analyzed by JSM-5410 LV scanning electron microscope with 20 kV of acceleration. All samples were coated with sputter gold under vacuum for conductivity.

2.3.5 Inductively coupled plasma-optical emission spectrometry (ICP-OES)

For analyzing metal content in the samples use the Thermo Scientific, iCAP Qc inductively coupled plasma-optical emission spectrometer. For analysis preparation, 0.0400 g of calcined catalyst was soaking with 10 mL of con. HCl and subsequently 10 mL of HF was added dropwise to get rid off silica in the form of volatile SiF₄. The sample was heated but not boiled until dryness on a hot plate and the fluoride treatment was repeated twice more. An amount of 10 mL of a mixture of 6 M HCl : 6 M HNO₃ at a ratio of 1: 3 was added slowly and warmed until dryness again. An amount of 10 mL deionized water was added to and warmed about 5 min to complete dissolution. The solution was transferred to a 50 mL polypropylene volumetric flask and shaken thoroughly. The solution was transferred into a plastic bottle with a treaded cap lined under with a polyethylene seal.

2.4 Procedure in oxidation reaction of benzene

The catalytic activity was investigated in oxidation reaction of benzene using H_2O_2 as an oxidant. The procedure was carried out in a three-necked round bottomed flask connected with a reflux condenser. A typical reaction was carried out as the follows: 0.075 g of catalyst, 1.75 g of benzene (22.4 mmol) and 5.66 g of acetonitrile were added into the flask. After heating the mixture to set temperature at 55°C , 30 wt.% of hydrogen peroxide (benzene: H_2O_2 mole ratio=1:3) was added dropwise. Then, the reaction mixtures were further stirred 3 h. After reaction, the catalysts were separated from the reaction mixture by centrifugation. The resulting products and unreacted substrate were extracted by diethyl ether 50 ml. The extracted liquid mixture was analyzed by gas chromatography.

2.5 Procedure in oxidation reaction of naphthalene

The catalytic activity was investigated in oxidation reaction of naphthalene using H_2O_2 as an oxidant. The procedure was carried out in a three-necked round bottomed flask connected with a reflux condenser. A typical reaction was carried out as the follows: 0.1 g of catalyst, 2.871 g of naphthalene (22.4 mmol) and 7.84 g of acetonitrile were added into the flask. After heating the mixture to set temperature at 60°C , 30 wt.% of hydrogen peroxide (naphthalene: H_2O_2 mole ratio=1:3) was added dropwise. Then, the reaction mixtures were further stirred 3 h. After reaction, the catalysts were separated from the reaction mixture by centrifugation. The resulting products and unreacted substrate were extracted by diethyl ether 50 ml. The extracted liquid mixture was analyzed by gas chromatography.

2.6 Iodometric titration process

2.6.1 Standardization of Sodium Thiosulfate

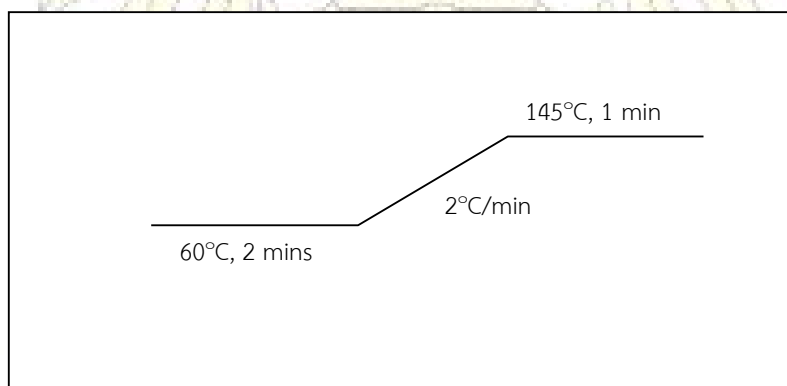
Pipette 20 mL of potassium iodate solution (0.1 N) into Erlenmeyer flask containing 100 mL of H_2O . After that, 20 mL of potassium iodide solution (0.1 N) was added and mixed well following the adding of 25 mL of acid mixture, stoppered the flask, and kept for five minutes. Then, solution mixture titrated with the sodium thiosulfate solution until the brown triiodide color is nearly dispersed to a pale straw color. 1 mL of Starch solution was added and then titrated until the solution changes sharply from blue to colorless. The titration volume was recorded, calculated the normality of the sodium thiosulfate solution and repeated procedure two additional times.

2.6.2 Determination of Hydrogen Peroxide

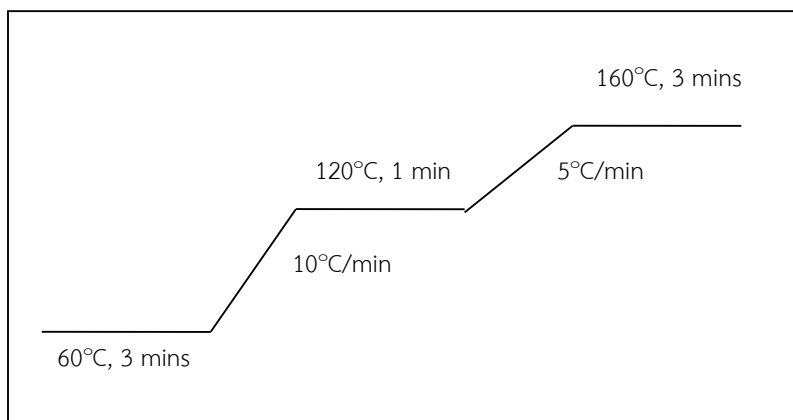
3 g of sample was loaded into Erlenmeyer flask. After that, 200 mL of water, 20 mL of potassium iodide solution, and 25 mL of the acid mixture (ammonium molybdate and conc. H_2SO_4) were added. The resulting solution was mixed, stoppered, and kept for five minutes. Then, the solution was titrated with sodium thiosulfate solution (0.1N) until the brown color of triiodide was reduced to a light straw color. The starch solution was added into the solution and then continued titrating until the blue color of the solution changed to colorless. The titration procedure was repeated without the addition of sample and recorded as blank titration volume [24].

2.7 Gas chromatography analysis (GC)

The phenol yield can be analyzed by gas chromatography which was carried out on a Varian CP 3800 gas chromatograph equipped with a 25 m length \times 0.32 mm inner diameter of HP-1 capillary column was used to analyze reaction mixture from benzene hydroxylation. Cycloheptanone was used as an internal standard and tetrahydrofuran as a solvent for analysis. The liquid sample volume was 1 μL . Flame ionization detector (FID) was used as a detector. The temperature program of column oven of benzene was illustrated in scheme 2.4 and the temperature program of naphthalene showed in scheme 2.5.



Scheme 2.4 The temperature program of benzene used for gas chromatography analysis.



Scheme 2.5 The temperature program of naphthalene used for gas chromatography analysis.



CHAPTER III
RESULTS AND DISCUSSION

3.1 Catalysts characterization

3.1.1 X-ray diffraction

3.1.1.1 TS-1

The low-angle XRD patterns of TS-1, vanadium metal supports on TS-1 and acid treated TS-1 were shown in Figure 3.1.1. The pattern of all materials was similar to typical pattern of MFI structure [25]. The results showed sharp peaks at $2\theta = 7.9, 8.9, 23.0, 23.9$ and 24.41 corresponding to the five characteristic peaks of MFI structure. The single diffraction peaks at $2\theta = 24.08$ and 30.34 should be due to the Ti-atom incorporated into the zeolite framework. After vanadium impregnation, the XRD pattern was still remained during the preparation of modified metal catalysts. Furthermore, the crystallinity of bimetallic catalysts showed lower intensity than TS-1. Moreover, the wide-angle XRD patterns of the catalysts are shown in Figure 3.12. From the result, the XRD pattern of the catalysts does not show the characteristic diffraction peak of V_xO_y phase.

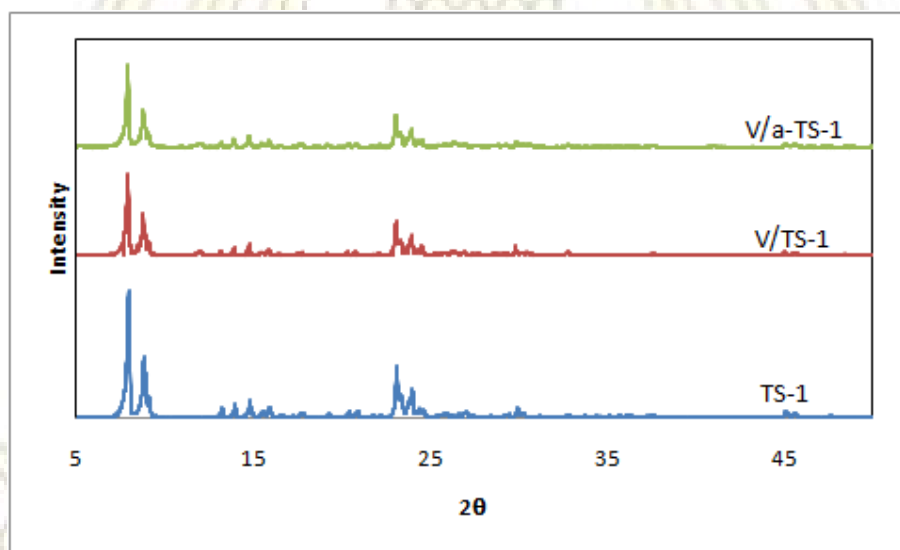


Figure 3.1.1 XRD patterns of bimetallic titaniumsilicalite-1 (V/TS-1) in the range of low-angle

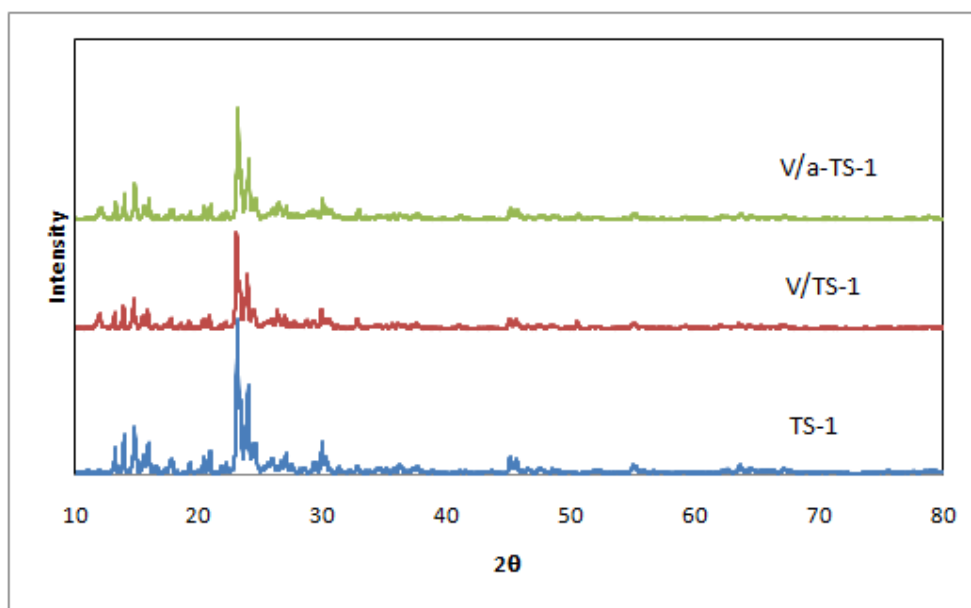


Figure 3.1.2 XRD patterns of bimetallic titaniumsilicalite-1 (V/TS-1) in the range of wide-angle

3.1.1.2 Ti-MCA

Figure 3.2(a) showed XRD patterns of Ti-MCA, vanadium metal supported on Ti-MCA and vanadium metal supported on acid treated Ti-MCA. The pattern of all materials was similar to the typical low angle XRD pattern of cubic Ia-3d structure. From the results, that showed two diffraction peaks as (211) and (220) plane in the range of $2\theta = 0.7\text{-}3.0^\circ$. These results suggested that the cubic Ia-3d structure of Ti-MCA was still remained during the preparation of bimetallic catalysts. In addition, the peak intensity of bimetallic catalysts was found to be decreased because of reducing of crystallinity. Moreover, the wide-angle XRD patterns of the catalysts are shown in Figure 3.2(b). For V/a-Ti-MCA, the characteristic diffraction peaks of V_2O_5 were at $2\theta = 15.56, 20.36, 31.58$ and 34.72° while V/Ti-MCA does not show the characteristic diffraction peak of V_xO_y phase [26]. This result indicated that V-species in Ti-MCA are higher dispersion on the surface of material. Furthermore, XRD spectra of V/a-Ti-MCA show the characteristic peak of the anatase phase at $2\theta \approx 26.3^\circ$ [27].

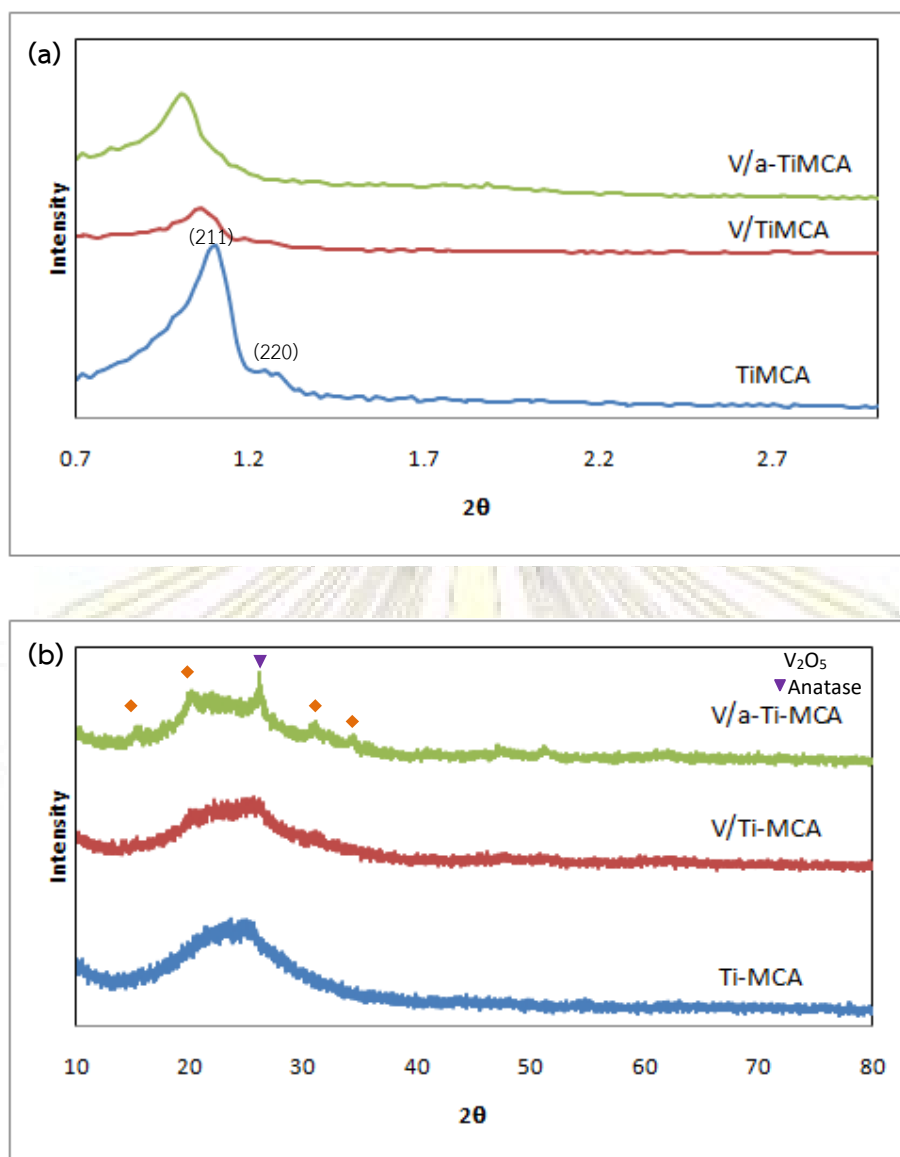


Figure 3.2 XRD patterns of bimetallic Ti-MCA (V/Ti-MCA) in the range of (a) low-angle and (b) wide-angle

3.1.2 DR-UV results

DR-UV spectra of TS-1 and Ti-MCA (in Figure 3.3) showed the absorption peaks at 210 and 320 nm. Usually, the strong peak at 210 nm can be ascribed to a charge transfer from oxygen to tetraordinated titanium and the peak at 320 nm was attributed to anatase phase titanium atom located at the tetrahedrally coordinating position in the framework of TS-1 [28]. After addition of secondary metal, an intense of absorption peak at about 210 nm attributed to the tetrahedrally coordinated titanium was detected in all the samples. Moreover, the spectrum of V/TS-1, V/a-TS-1, V/Ti-MCA and V/a-Ti-MCA showed the absorption

bands at 210, 280, 340, 380, 420, 460 and 500 nm. The peaks at 210 and 280 nm can be attributed to the isolated tetrahedral V^{5+} species, while two absorption peaks at 340 and 380 nm indicated the presence of low oligomeric tetrahedral coordinated V^{5+} species [29]. Moreover, the absorption peak at 420 nm corresponding to the octahedral V^{5+} species, as well as the absorption region at 450-550 nm associated to bulk V_2O_5 . Therefore, the results suggested the VO_x structure can be present in the form of tetrahedral VO_4 species, low polymeric and crystalline V_2O_5 .

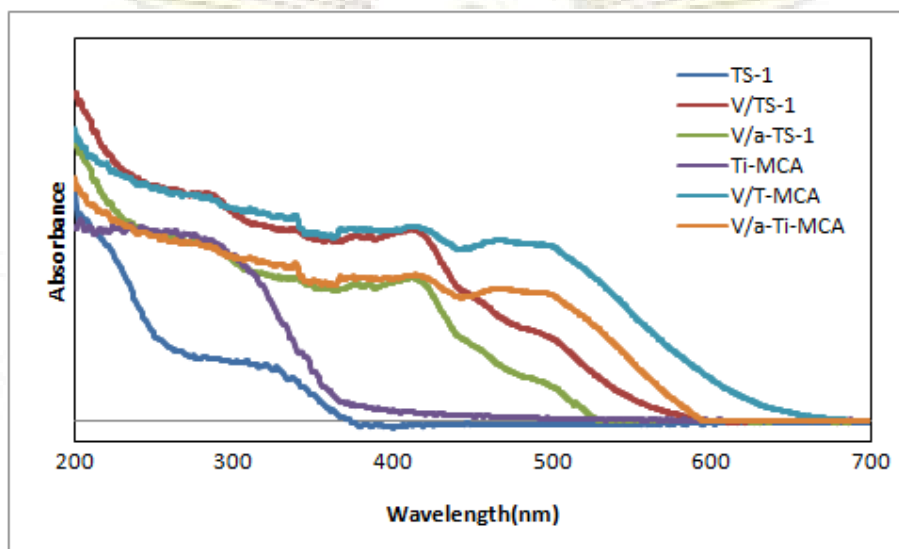


Figure 3.3 DR-UV spectra of V/TS-1 and V/Ti-MCA

3.1.3 N_2 sorption properties

3.1.3.1 TS-1

The nitrogen adsorption/desorption isotherms of TS-1 and vanadium supported on TS-1 catalyst were shown in Figure 3.4. It is clear that the nitrogen adsorption/desorption isotherms of TS-1 showed the typical type I as defined by IUPAC for microporous materials and a placid hysteresis loop with a small closed area. After the impregnation of vanadium metal, the isotherms of V/TS-1 and V/a-TS-1 catalysts retained their shape, which could be an indication for maintenance of the microscopic order of the parent material. The samples exhibited pore size distribution centered mostly at 0.6 nm. The physical properties of the samples were summarized in Table 3.1. From the results, the surface area and pore volume were sharply decreased after the addition of vanadium. This result indicated that a portion of the metal oxide particles have entered into the pores leading to partial blockage by some agglomerates.

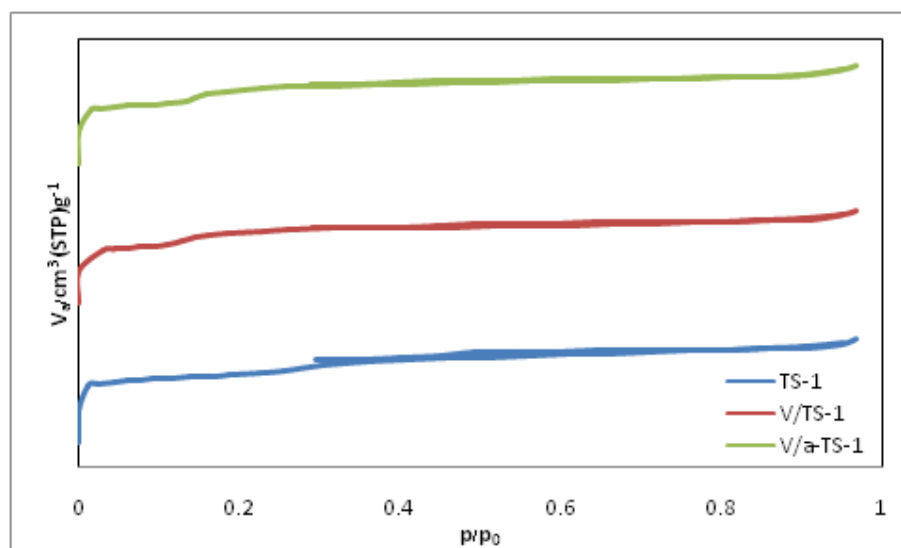


Figure 3.4 N₂ adsorption/desorption isotherms of bimetallic TS-1

3.1.3.2 Ti-MCA

The nitrogen adsorption/desorption isotherms of metal supported on Ti-MCA were shown in Figure 3.5. All samples displayed isotherms type IV which is the characteristics of mesoporous materials. The results indicated that the mesostructured materials were preserved after metal impregnation and calcination. The vanadium-modified and acid treated catalysts exhibited pore size distribution having size around 5.4-7.0 nm whereas a parent Ti-MCA showed the narrow pore size distribution centered mostly at 5.4 nm. Furthermore, the surface properties of prepared catalysts are summarized in Table 3.1. The total specific surface area and pore volume of bimetallic catalysts was drastically reduced in comparison with Ti-MCA. This result indicated that the metal oxide particles could be placed in the pores or coating the inner walls of Ti-MCA.

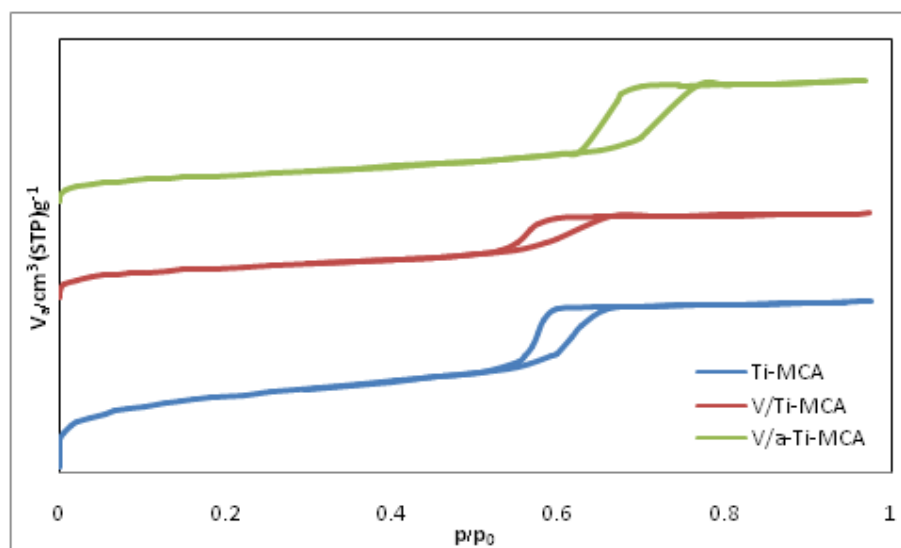


Figure 3.5 N_2 adsorption/desorption isotherms of bimetallic Ti-MCA

Table 3.1 Textural properties of vanadium supported of TS-1 and Ti-MCA materials.

Catalyst	N_2 Adsorption / desorption		
	Specific surface area (BET) (m^2g^{-1})	Pore volume (cm^3g^{-1})	Pore diameter (nm)
TS-1	321	0.17	0.6
V/TS-1	311	0.15	0.6
V/a-TS-1	311	0.16	0.6
Ti-MCA	1138	0.92	5.4
V/Ti-MCA	547	0.52	5.4
V/a-Ti-MCA	487	0.80	7.0

3.1.4 SEM images

The SEM images and EDX map of vanadium supported on TS-1, a-TS-1, Ti-MCA and a-Ti-MCA samples were shown in Figure 3.6. The surface of V/a-TS-1 and V/a-Ti-MCA showed rougher than V/TS-1 and V/Ti-MCA, respectively, because acid treatment affected the morphology of catalysts. Moreover, from the EDX images showed the well dispersion of titanium and vanadium in composite catalysts.

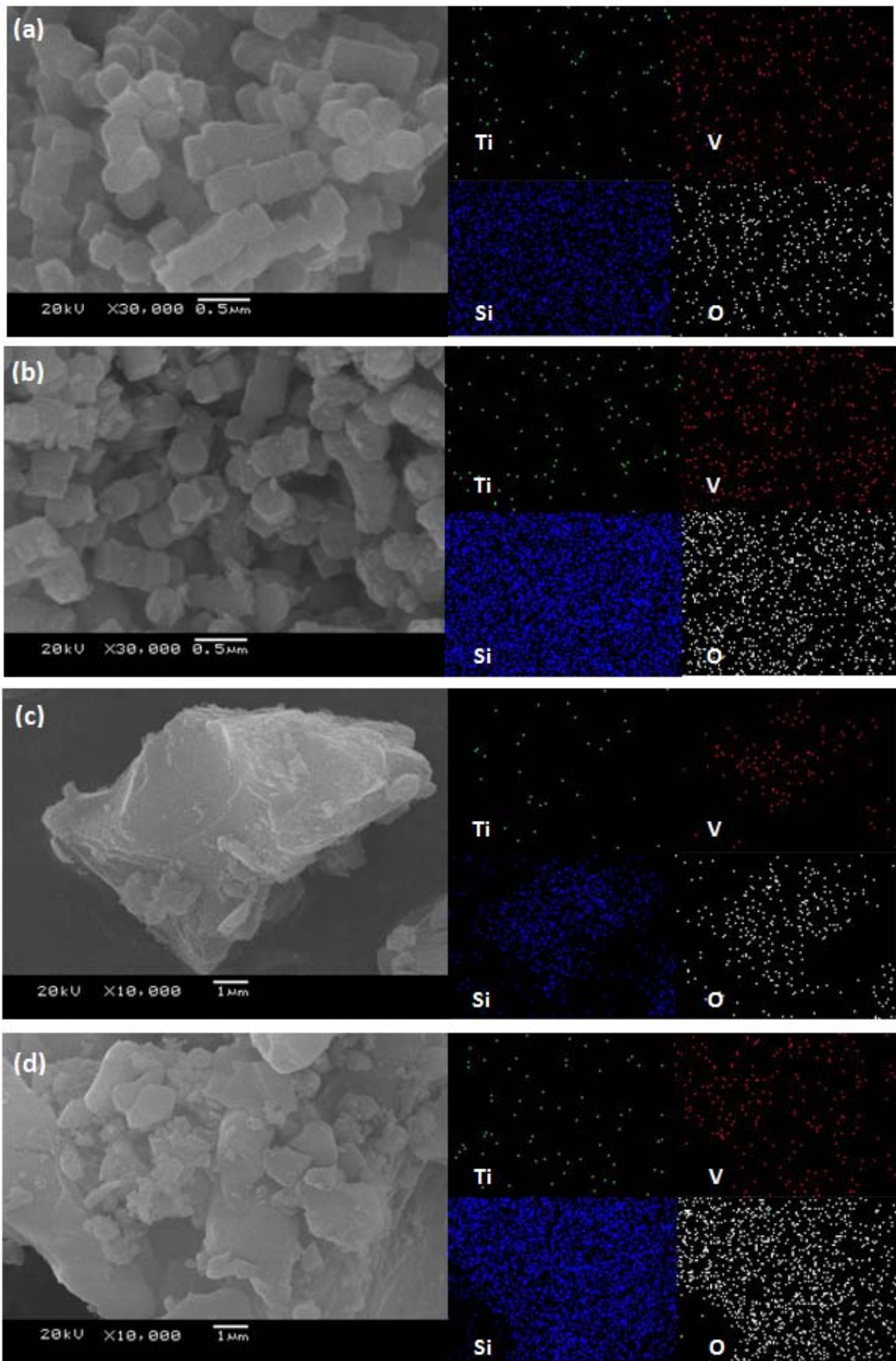


Figure 3.6 SEM images and EDX maps of composite elements Ti, V, Si, O of (a) V/TS-1, (b) V/a-TS-1, (c) V/Ti-MCA and (d) V/a-Ti-MCA.

3.1.5 ICP-OES results

The content of metals was determined by using Inductively Coupled Plasma - optical emission spectrometer (ICP-OES). The elemental analysis data of transition-metal titanosilicate catalysts are shown in Table 3.2. The ICP-OES analysis showed a higher deviation of Si/Ti mole ratio than the amount of metal in solution loading (Si/Ti mole ratio = 40) due to remaining Ti in the synthetic gel. Furthermore, acid treatment could removed a part of titanium from TS-1 and Ti-MCA. Moreover, the amount of vanadium was closed to stoichiometric adding values as 10 wt.% of both TS-1 and Ti-MCA sample.

Table 3.2 Metal content analysis of V/TS-1 and V/Ti-MCA with different V-content.

Catalyst	Si/Ti mole ratio ^a	V-content (wt.%) ^a
TS-1	65.74	-
V/TS-1	57.46	10.97
V/a-TS-1	73.82	10.53
Ti-MCA	87.41	-
V/Ti-MCA	89.69	10.03
V/a-Ti-MCA	108.65	10.23

^a Inductively coupled plasma-optical emission spectrometry

3.2 Oxidation reaction of benzene and naphthalene

The oxidation reaction of benzene and naphthalene were carried out with varying type of catalysts such as TS-1, V/TS-1, V/a-TS-1, Ti-MCA, V/Ti-MCA and V/a-Ti-MCA. The results were summarized in Table 3.3. For the prepared catalysts, vanadium oxide in catalysts was the catalytic active site for oxidation of benzene and naphthalene because V^{5+} was lewis acid. Therefore, another important factor affecting the catalytic performance was their structure of catalyst support. From the results, it was found that V/Ti-MCA gave higher %yield of phenol and %conversion of naphthalene than other catalysts. Although TS-1 was well known as effective redox catalyst showed a lowest yield of phenol and conversion of naphthalene. This result caused by small pore size that led to mass transport limitation resulting in a lower catalytic activity than other catalysts, when compared with Ti-MCA is larger pore size than TS-1. Furthermore, vanadium supported on Ti-MCA was more active than vanadium supported on acid treated Ti-MCA by showing the phenol yield of 14.0% and the naphthalene conversion of 34.0% because of the higher amount of Ti content in V/Ti-MCA.

Table 3.3 Catalytic activity of vanadium-titanosilicate catalysts for the oxidation reaction of benzene and naphthalene

Catalyst	Benzene ^b		Naphthalene ^c	
	%yield Phenol	H ₂ O ₂ ^a efficiency	%conversion Naphthalene	H ₂ O ₂ ^a efficiency
TS-1	0.3	24	7.0	23
V/TS-1	9.0	89	20.2	91
V/a-TS-1	8.2	78	7.9	75
Ti-MCA	0.5	28	8.0	24
V/Ti-MCA	14.0	100	34.0	100
V/a-Ti-MCA	13.5	100	30.8	100

^a H₂O₂ efficiency = (mole of H₂O₂ decomposed/starting mole of H₂O₂) x100

^b Benzene reaction condition: 0.075 g of catalysts, acetonitrile 5.66 g, benzene:H₂O₂ = 1:3, 55°C, 3 h.

^c Naphthalene reaction condition: 0.1 g of catalysts, acetonitrile 7.84 g, naphthalene:H₂O₂ = 1:3, 60°C, 3 h.

CHAPTER IV

CONCLUSIONS

The transition metal-titanosilicates with the vanadium metal were successfully synthesized by hydrothermal followed by impregnation method. All synthesized materials were characterized by X-ray powder diffraction, N_2 adsorption-desorption, DR-UV spectroscopy, SEM-DEX and ICP-OES. The XRD analysis of all catalysts indicated the characteristic peak of each parent material. In addition, the results of vanadium phase are in a good agreement with the results from DR-UV spectroscopy. N_2 adsorption-desorption isotherms exhibited a type I according to the IUPAC classification for microporous material for TS-1 and type IV, which referred to typical shape of mesoporous structures for Ti-MCA. Amount of vanadium in catalysts were determined by using ICP-OES which there are about 10%wt.

In the oxidation of benzene and naphthalene, the reactions were carried out by varying catalyst types including TS-1, V/TS-1, V/a-TS-1, Ti-MCA, V/Ti-MCA and V/a-Ti-MCA by using hydrogen peroxide as an oxidant. It was found that V/Ti-MCA showed highest catalytic performance with 14.0% yield of phenol. The condition of benzene oxidation was carried at benzene: H_2O_2 mole ratio of 1:3, 0.075 g of catalyst, acetonitrile 5.66 g, 55°C for 3 h. Moreover, the conversion of naphthalene over the same catalyst as 34.0% with condition at naphthalene: H_2O_2 mole ratio of 1:3, 0.1 g of catalyst, acetonitrile 7.84 g, 60°C for 3 h.

REFERENCES

- 1 Use of phenol [Online]. Available from:
<http://www.essentialchemicalindustry.org/chemicals/phenol.html> [18 April]
- 2 Global phthalic anhydride market [Online]. Available from:
<https://www.transparencymarketresearch.com/pressrelease/phthalic-anhydride.htm>
[18 April]
- 3 XU, D.; JIA, L.; GUO, X. Cu-doped mesoporous VO_x-TiO₂ in catalytic hydroxylation of benzene to phenol. *Chinese Journal of Catalysis* . **2013**, *34*, 341–350.
- 4 Xiangju, Y.; Yanjuan, C.; Xiaoqing, Q.; Xinchun, W. Selective oxidation of benzene to phenol by Fe-CN/TS-1 catalysts under visible light irradiation. *Applied Catalysis B: Environmental*. **2014**, *152–153*, 383–389.
- 5 Yuma, M.; Shuji, B.; Nobutaka, F.; Hideki, S.; Shinobu, I. Direct Hydroxylation of Benzene to Phenol Using Hydrogen Peroxide Catalyzed by Nickel Complexes Supported by Pyridylalkylamine Ligands. *J. Am. Chem. Soc.* **2015**, *137*, 5867-5870.
- 6 Feng, S.; Man, K. T.; Matthias, B. Selective oxidation of naphthalene derivatives with ruthenium catalysts using hydrogen peroxide as terminal oxidant. *Journal of Molecular Catalysis A: Chemical*. **2007**, *270*, 68–75.
- 7 Adrienn, B.; Janos, H. OXIDATION OF CONDENSED CYCLIC HYDROCARBONS WITH H₂O₂ IN THE PRESENCE OF MODIFIED MCM-41 AND SBA-15 MESOPOROUS CATALYSTS. *React.Kinet.Catal.Lett.* **2009**, *96*, 413-420.
- 8 Zhai, Z.; Yang, Y.; Juan, Q.; Jiaqi, Z.; Fulin, C.; Wemliang, W. Liquid-phase oxidation of naphthalene with H₂O₂ in the presence of ordered mesoporous V-m-Al₂O₃ catalysts. *J. Chem. Sci.* **2017**, *129*, 1373–1380.
- 9 The effect of a catalyst on the activation energy of a reaction [Online]. Available from: <https://archive.cnx.org/contents/ea93e564-1498-4e31-9c4e-3aba71467a82@2/>
reaction-rates [18 April]
- 10 Types of catalysts [Online]. Available from:
<https://www.chemguide.co.uk/physical/catalysis/introduction.html> [18 April]

- 11 Microporous material [Online]. Available from:
https://en.wikipedia.org/wiki/Microporous_material [18 April]
- 12 MFI structure [Online]. Available from:
<http://asia.iza-structure.org/IZA-SC/framework.php?STC=MFI> [18 April]
- 13 Khouw, C.B.; Dartt, C.B.; Labinger, J.A.; Davis, M.E. Studies on the Catalytic Oxidation of Alkanes and Alkenes by Titanium Silicates. *Journal of Catalysis*. **1994**, *149*, 195-205.
- 14 Bianchi, D.; D'Aloisio, R.; Bortolo, R.; Ricci, M. Oxidation of mono- and bicyclic aromatic compounds with hydrogen peroxide catalyzed by titanium silicalites TS-1 and TS-1B. *Applied Catalysis A: General*. **2007**, *327*, 295-299.
- 15 Kubota, Y.; Jin, C.; Tatsumi, T. Performance of organic-inorganic hybrid catalysts based on la-3d mesoporous silica. *Catalysis Today*. **2008**, *132*, 75-80.
- 16 Wang, S.; Wu, D.; Sun, Y.; Zhong, B. The Synthesis of MCM-48 with high yields. *Materials Research Bulletin*. **2001**, *36*, 1717-1720.
- 17 Diffraction of x-rays by crystals [Online]. Available from:
<http://www.kshitijitjee.com/diffraction-of-x-rays-by-crystals/> [18 April]
- 18 The IUPAC classification of adsorption isotherm [Online]. Available from:
<http://www.microtrac-bel.com/en/tech/bel/seminar02.html> [18 April]
- 19 Principle of Scanning Electron Microscope (SEM) [Online]. Available from:
<https://sites.google.com/site/frontierlab2011/scannig-electron-microscope/principie-of-sem> [18 April]
- 20 Major components and ICP-OES instrument [Online]. Available from:
<http://analyticalprofessional.blogspot.com/2013/06/inductive-coupled-plasma-optical.html> [18 April]
- 21 Oxidation [Online]. Available from: <https://simple.wikipedia.org/wiki/Oxidation> [18 April]
- 22 Xiang, S. W.; Xin, W. G.; Gang, L. Synthesis of titanium silicalite (TS-1) from the TPABr system and its catalytic properties for epoxidation of propylene. *Catalysis Today*. **2002**, *74*, 65-75.

- 23 Kubota, Y.; Jin, C.; Tatsumi, T. Performance of organic–inorganic hybrid catalysts based on la-3d mesoporous silica. *Catalysis Today*. **2008**, *132*, 75-80.
- 24 Determination of Hydrogen Peroxide Concentration [Online]. Available from: www.sciencemadness.org/talk/files.php?pid=317389&aid=29281 [18 April]
- 25 Yeong, Y.F.; Abdullah, A.Z.; Ahmad, A.L.; Bhatia, S. Synthesis, structure and acid characteristics of partially crystalline silicalite-1 based materials. *Microporous and Mesoporous Materials*. **2009**, *123*, 129-139.
- 26 Kaid, M.A. Characterization of Electrochromic Vanadium Pentoxide Thin Films Prepared By Spray Pyrolysis. *Egypt. J. Solids*. **2006**, *29*, 273-291.
- 27 Bandas, C.; Lazau, C.; Dabici, A.; Sfirloaga, P.; Vaszilcsin, N.; Grozescu, I.; Tiponut, V. Microwave-Assisted Hydrothermal Method for Synthesis of Nanocrystalline Anatase TiO₂. *Chem. Bull.* **2011**, *56*, 81-84.
- 28 Lv, Q.; Li, G.; Sun, H. Synthesis of hierarchical TS-1 with convenient separation and the application for the oxidative desulfurization of bulky and small reactants. *Fuel*. **2014**, *130*, 70-75.
- 29 Hassan, Z. M. Javaid, S. M.; Kaliaguine, S. Comparative study of vanadium aluminophosphate molecular sieves VAPO-5, -11, -17 and - 31. *Applied Catalysis A: General*. **2000**, *196*, 9-24.



APPENDICES

1. Iodometric titration

1.1 Standardization of Sodium Thiosulfate

$$\text{Normality of sodium thiosulfate solution} = \frac{(\text{g KIO}_3)(\text{mL KIO}_3)}{(\text{mL Na}_2\text{S}_2\text{O}_3)(35.67 \text{ g.L / eq})}$$

1.2 Determination of Hydrogen Peroxide

$$\text{Hydrogen peroxide \% w/w} = \frac{(A-B)(N)(1.7007)}{\text{Sample Weight}}$$

Where: A = Titration volume for sample

B = Titration volume for blank.

N = Normality of $\text{Na}_2\text{S}_2\text{O}_3$

2. Calculation of % phenol yield

$$\% \text{ yield} = \frac{\text{mole of phenol formed}}{\text{initial mole of benzene}} \times 100$$

3. Calculation of % naphthalene conversion

$$\% \text{ conversion} = \frac{(\text{initial mole of naphthalene} - \text{final mole of naphthalene}) \times 100}{\text{initial mole of naphthalene}}$$

4. Phenol calibration curve

The concentrations of phenol were prepared as 0.015 M, 0.025 M and 0.075 M. The standard calibration curve of phenol was shown in Figure A-1. The standard curve equation is expressed as following

$$y = 1.360x - 0.014$$

where

y is mole phenol/mole IS

x is area phenol/area IS

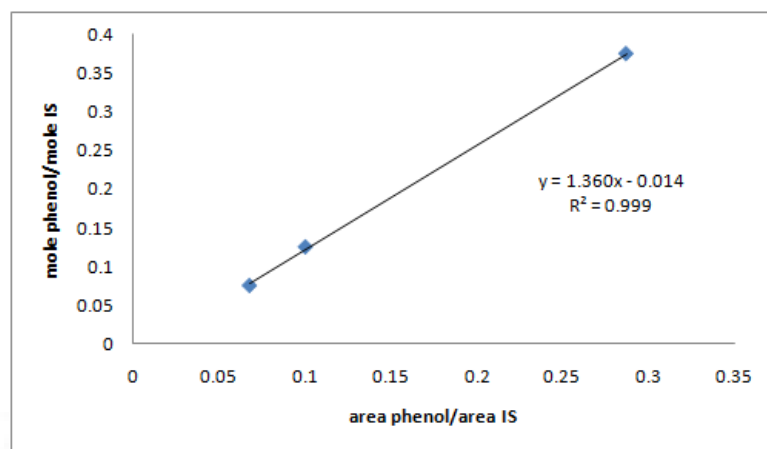


Figure A-1 Calibration curve of phenol

5. Naphthalene calibration curve

The concentrations of naphthalene were prepared as 0.1 M, 0.41 M and 0.6 M. The standard calibration curve of naphthalene was shown in Figure A-2. The standard curve equation is expressed as following

$$y = 1.143x - 0.381$$

where

y is mole naphthalene /mole IS

x is area naphthalene /area IS

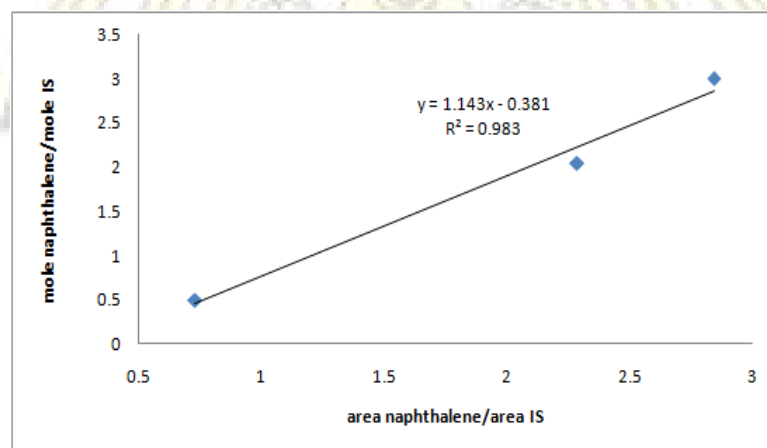


Figure A-2 Calibration curve of naphthalene

VITAE

Miss Savitree Phengboon was born on June 25, 1996 in Singburi, Thailand. She graduated high school in Gifted Program from Singburi School in 2013. After that, she continued her study in Department of Chemistry, Faculty of Science, Chulalongkorn University in 2014. Her present address is 89 Moo 3, Tumbon Phokruam, Amphur Muang, Singburi 16000. E-mail address is Savitree_Eed@hotmail.com.

